# Robust Design of Countercurrent Adsorption Separation Processes: 4. Desorbent in the Feed

**Marco Mazzotti**
Dipt. di Chimica, Politecnico di Milano, I20131 Milano, Italy

**Giuseppe Storti**
Dipt. di Ingegneria Chimica e Materiali, Università degli Studi di Cagliari, I09123 Cagliari, Italy

**Massimo Morbidelli**
Laboratorium für Technische Chemie LTC, ETH Zentrum, CH-8092 Zürich, Switzerland

*In many instances of practical interest, countercurrent adsorption separations operate on feed streams containing not only the components to be separated but also some desorbent. Criteria for the optimal and robust design and operation of these units are developed by extending previous treatments developed for desorbent-free feedstreams. The effect of the presence of some desorbent (weak, intermediate, or strong) on the location and robustness of the region of complete separation in the operating parameter space is discussed.*

## Introduction and Motivation

The adsorptive separation of multicomponent mixtures can be accomplished in units where the countercurrent contact between the fluid and the adsorbed phase is achieved either in a true countercurrent mode (true countercurrent (TCC) units) or in a simulated fashion (simulated moving-bed (SMB) units; cf. Ruthven, 1984; Ganetsos and Barker, 1993). Even though SMB units are mostly used in applications (see, for example, various hydrocarbon, sugar and enantiomer mixtures separations), the equivalent TCC configuration is most conveniently referred to for design purposes. This is possible due to the well-established equivalence between TCC and SMB configurations (cf. Ruthven and Ching, 1989).

A scheme of the classic four-section TCC unit is shown in Figure 1. Actually, also three-section units (without section 4, where the desorbent is regenerated) and two-section units (where section 1 is also absent and the adsorbent is not recycled) are often used in applications (cf. Ching et al., 1992, for an application of three- and four-section configurations to sugar separation, and Baciocchi et al., 1996, for the application of a three-section SMB to the separation of a $C_5$ mixture in the vapor phase). All these configurations can be analyzed following the same approach. Typically, using a proper desorbent complete separation is sought, where the most adsorbable components of the feed are collected in the extract stream, and the least adsorbable ones in the raffinate. Complete separation is achieved when both outlet streams exhibit 100% purity, that is, strong and weak components are absent from raffinate and extract, respectively. Both extract and raffinate streams contain some desorbent, which is removed afterwards, in most cases by distillation, and then recycled back to the adsorptive separation unit.

The operating conditions needed to achieve the desired separation performance can be selected through the proper criteria, which were developed in the first parts of this series

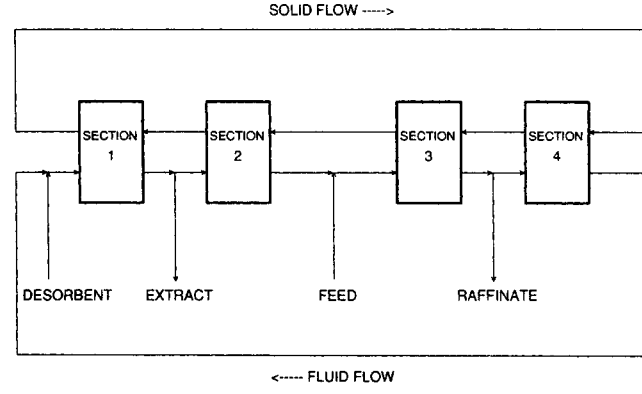


**Figure 1. Four-section true countercurrent separation.**

Correspondence concerning this article should be addressed to M. Morbidelli.

(Storti et al., 1993; Mazzotti et al., 1994, 1996). These are based on the equilibrium theory model (cf. Helfferich and Klein, 1970 and Rhee et al., 1971, who apply the $h$- and $\omega$-transformations, respectively; see also Helfferich, 1991, who proves the equivalence of the two approaches), where dissipative phenomena, namely, axial mixing and mass-transport resistances, are neglected and adsorption equilibrium is assumed to be established everywhere at every time in the column. It has been demonstrated that the key operating parameters in determining the steady-state separation performance are the flow-rate ratios, $m_j$, in the different sections of the unit. These are defined as follows:

$$m_j = \frac{\text{net fluid flow rate}}{\text{adsorbed-phase flow rate}} = \frac{u_j \rho_f - u_s \epsilon_p \rho_f}{u_s \rho_s \Gamma^\infty (1-\epsilon_p)} = \frac{G_j t^* - AL\epsilon^* \rho_f}{AL\rho_s \Gamma^\infty (1-\epsilon^*)}, \quad (1)$$

where all the symbols are defined in the "Notation" section and the second equality refers to TCC units, whereas the rightmost one applies to SMB units. The two expressions of $m_j$ are related by the conversion rules between SMB and TCC units, based on their kinematic equivalence (cf. Mazzotti et al., 1994).

These criteria provide the boundaries of the complete separation region in the space spanned by the operating parameters $m_j$ (the dimension of this space equals the number of sections of the separation unit). This region is constituted of operating points for which in the frame of equilibrium theory complete separation, in the sense defined earlier, is achieved. The graphical representation of its projection onto the plane $(m_2, m_3)$ is very useful to determine optimal and robust operating conditions (Storti et al., 1993, 1995). The approach can be applied to the separation of both binary and multicomponent feed mixtures (Mazzotti et al., 1994).

In the previous parts of this series optimal design criteria have been developed for systems described by adsorption isotherms of the general form:

$$\theta_i = \frac{\Gamma_i}{\Gamma^\infty} = \frac{(\Gamma_i^\infty/\Gamma^\infty) K_i c_i}{\delta} = \frac{(\Gamma_i^\infty/\Gamma^\infty) \rho_f K_i y_i}{\delta}, \quad (2)$$

which for $\delta = 1$ reduces to the linear system $\theta_i = H_i y_i$, for $\delta = \rho_f \sum_{l=1}^{NC} K_l y_l$, and $\Gamma_i^\infty = \Gamma^\infty$ represents the stoichiometric Langmuir isotherm and for $\delta = 1 + \rho_f \sum_{l=1}^{NC} K_l y_l$ it represents the nonstoichiometric Langmuir isotherm. These three adsorption equilibrium isotherms are capable of describing a large class of systems of practical interest.

In all cases only bulk separations have been considered, where no desorbent is present in the feed stream, which is assumed to be constituted only of the components to be separated. Even though this is the case in some classic applications of the SMB technology, such as, for example, xylene separation, it is certainly not true in many other situations of interest, in particular in the fine chemical, food, and pharmaceutical industries as discussed in detail next.

Let us first consider a multicomponent mixture that must be separated into a number $NF$ of fractions, with $NF > 2$. As in the case of distillation, a cascade of $(NF-1)$ countercurrent adsorptive separation units, most likely SMB units, is required. In particular, let $NF = 3$; in this case, two SMB units and three final separation units, typically distillation columns, are involved. The feed mixture constituted of components $A$, $B$, and $C$ and a stream of desorbent are fed to the first SMB unit. One of the outlet streams, constituted of $C + D$, is sent to a distillation column, from which pure $C$ is obtained and the desorbent is recycled. The other outlet stream contains $A + B + D$ and represents the feed stream to the second SMB unit where $A$ and $B$ are separated. Therefore, the feed to the second SMB unit is constituted of the components to be separated, together with some desorbent, whose concentration can be rather high, depending on the enrichment achieved in the first SMB unit. Even though the possibility of separating $A + B$ from $D$ by distillation before feeding the second SMB unit should be considered, it may not be the most convenient solution, since it requires four distillation columns instead of three (one distillation column to separate $C$ from $D$, and two to separate $A$ from $D$ and $B$ from $D$, respectively, downstream of the second SMB unit).

The second situation to be considered, which is indeed the most common in applications, refers to the case where the components to be separated are dissolved in a solvent that can also be conveniently used as a desorbent. This is the case of a large class of separations of interest, mainly in the fine chemical, food, and pharmaceutical industries, as, for example, sugar (cf. Ching and Ruthven, 1985) and enantiomer separations (Negawa and Shoji, 1992; Ching et al., 1993; Nicoud et al., 1993; Küsters et al., 1995). If the product is highly diluted, then the linear theory can be applied and the results reported by Storti et al. (1993) can be used directly to determine the operating conditions needed to achieve complete separation (it is noteworthy that in the case of the separation of glucose and fructose on $Ca^{2+}$ ion-exchange resins the adsorption equilibrium isotherms are practically linear over a rather wide range of concentration, as reported by Ching and Ruthven, 1985). However, if this is not the case and the nonlinear character of the adsorption isotherm must be accounted for (Negawa and Shoji, 1992; Nicoud et al., 1993; Charton and Nicoud, 1995; Küsters et al., 1995), then the criterion for optimal design of the separation is currently available. In this article we derive such a criterion by extending and generalizing the results obtained in the previous articles of this series to the case where some desorbent is present in the feed stream.

## Operating Conditions for Complete Separation

In this section we develop the criteria for the choice of the operating conditions needed to achieve complete separation in the case where the feed stream contains not only the components to be separated but also some desorbent. To this aim we consider the separation of a binary mixture constituted of a stronger species $A$ and a weaker species $B$, using component $D$ as desorbent. The system is characterized by the stoichiometric Langmuir adsorption isotherm, involving only three equilibrium constants, namely $K_A$, $K_B$, and $K_D$, with $K_A > K_B$. The desorbent can have any adsorptivity value with respect to components $A$ and $B$, that is, it can be either weak, with $K_D < K_B < K_A$, or intermediate ($K_B < K_D < K_A$), or strong ($K_B < K_A < K_D$).

Thus, we are able to derive explicit expressions for the boundaries of the complete separation region in the operating parameter space, which provide quantitative and qualitative information about the separation performance. In the case of more complex systems (i.e., multicomponent or nonstoichiometric systems), these findings can be used on a qualitative basis to predict how the complete separation region obtained in the case of a desorbent-free feedstream changes when some desorbent is present in the feed. This follows from the evidence that as far as the shape of the complete separation region and its changes under the effect of changes of the system parameters (adsorptivity of the desorbent, feed composition, and so on) are concerned, multicomponent systems (Mazzotti et al., 1994) and systems described by the nonstoichiometric Langmuir isotherm (Mazzotti et al., 1996) behave qualitatively in the same way as binary systems characterized by the stoichiometric Langmuir isotherm. Thus, all that we learn by studying binary stoichiometric systems is very helpful, not only *per se* but also in analyzing several other systems, at least on a qualitative basis. A quantitative analysis of the effect of the presence of the desorbent in the feed in the case of the separation of multicomponent feedstreams and of mixtures characterized by the nonstoichiometric Langmuir isotherm can be performed by following the procedures described elsewhere (Mazzotti et al., 1994, 1996).

Let us first consider the case where adsorption of the feed components is described by the linear isotherm, $\theta_i = H_i y_i$. In this case, the constraints on the net flow-rate ratios depend on neither desorbent adsorptivity nor feed composition; hence, they do not change, whether or not the presence of the adsorbent in the feed is accounted for. These constraints are given by the following inequalities (Storti et al., 1993):

$$\begin{aligned} H_A &< m_1 < \infty \\ H_B &< m_2 < H_A \\ H_B &< m_3 < H_A \\ \frac{-\epsilon_p \rho_f}{\rho_s \Gamma^{\infty}(1-\epsilon_p)} &< m_4 < H_B. \end{aligned} \tag{3}$$

Let us now consider a system governed by the stoichiometric Langmuir adsorption isotherm. Accounting for the possible presence of the desorbent in the feed stream and following the procedure reported in the Appendix yields explicit expressions for the boundaries of the complete separation region in the operating parameter space.

In particular, in sections 1 and 4 the same constraints as those reported by Mazzotti et al. (1994) must be fulfilled:

$$\frac{K_A}{K_D} < m_1 < +\infty$$

(weak and intermediate desorbent) (4)

$$\frac{-\epsilon_p \rho_f}{\rho_s \Gamma^{\infty}(1-\epsilon_p)} < m_4 < \frac{K_B}{K_D}$$

(intermediate and strong desorbent) (5)

Note that in the case of strong and weak desorbent, the constraints on $m_1$ and $m_4$, respectively, were not reported before, since they are not explicit and actually involve all the other flow-rate ratios. Approximate conservative constraints are given by $m_1 > 1$ in the case of strong desorbent and $m_4 < 1$ in the case of weak desorbent.

The projections of the complete separation region onto the $(m_2, m_3)$ plane in the case of intermediate, weak, and strong desorbent are shown in Figures 2a, 2b and 2c, respectively. The equations representing the boundaries of these regions are given in explicit form in the following, where proper reference to the relevant figures is made.

- Straight line $WD$ (Figure 2a) and $W_sD$ (Figure 2c):

$$K_A(\Omega_G - K_B)m_2 + K_B(K_A - \Omega_G)m_3 = \Omega_G\Omega_H(K_A - K_B)/K_D. \tag{6}$$

- Straight line $WC$ (Figure 2a) and $W_wC$ (Figure 2b):

$$K_A(\Omega_H - K_B)m_2 + K_B(K_A - \Omega_H)m_3 = \Omega_G\Omega_H(K_A - K_B)/K_D. \tag{7}$$

- Straight line $W_wB$ (Figure 2b):

$$[K_D(K_A - K_B) - K_B(K_A - K_D)y_A^F]m_2 + K_B(K_A - K_D)y_A^F m_3 = K_B(K_A - K_B). \tag{8}$$

- Straight line $W_sA$ (Figure 2c):

$$K_A(K_D - K_B)y_B^F m_2 + [K_D(K_A - K_B) - K_A(K_D - K_B)y_B^F]m_3 = K_A(K_A - K_B). \tag{9}$$

- Curve $TA$ (Figures 2a and 2b):

$$m_3 = m_2 + \frac{\left(\sqrt{K_A} - \sqrt{K_D m_2}\right)^2}{y_A^F(K_A - K_D)}. \tag{10}$$

- Curves $RB$ (Figures 2a and 2c):

$$m_2 = m_3 - \frac{\left(\sqrt{K_B} - \sqrt{K_D m_3}\right)^2}{y_B^F(K_D - K_B)}. \tag{11}$$

- Straight line $AB$ (Figures 2a, 2b and 2c):

$$m_3 = m_2. \tag{12}$$

The coordinates of the intersection points are given by:

$$\text{point } A \quad \left(\frac{K_A}{K_D}, \frac{K_A}{K_D}\right) \tag{13}$$

$$\text{point } B \quad \left(\frac{K_B}{K_D}, \frac{K_B}{K_D}\right) \tag{14}$$

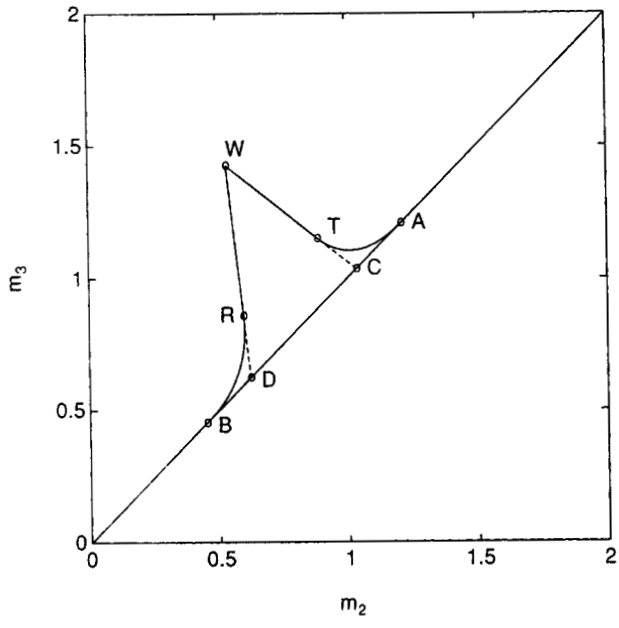


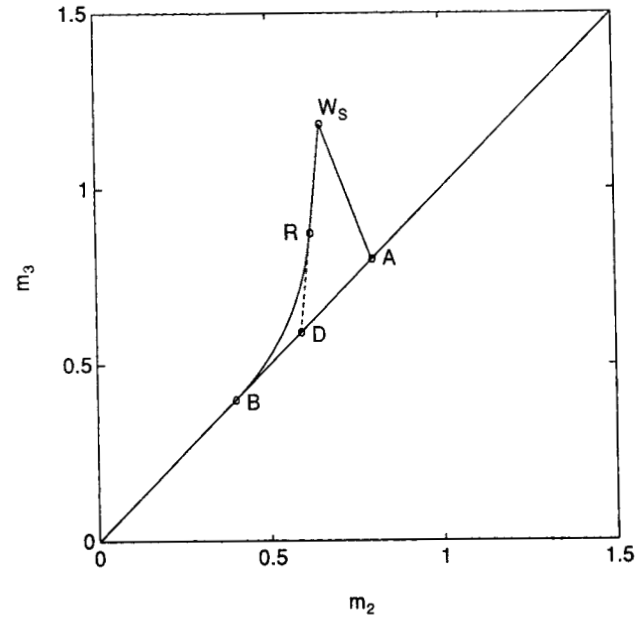


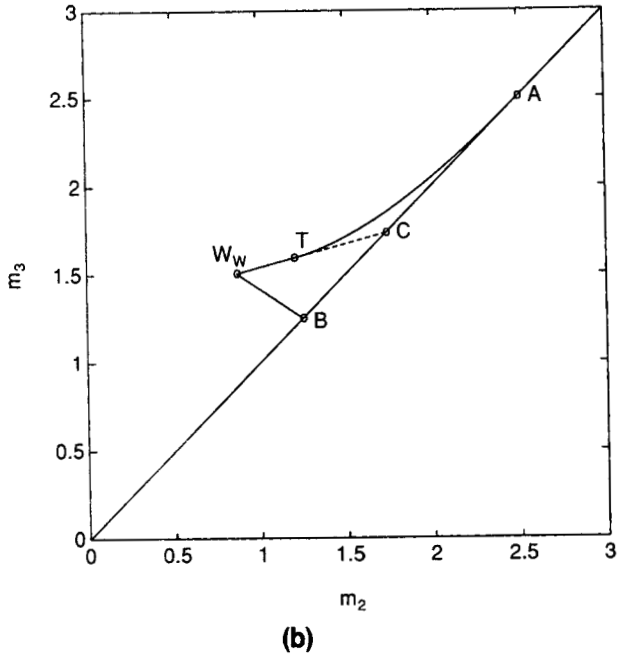


**Figure 2. Region of complete separation in the ($m_2$, $m_3$) plane.**

(a) Intermediate desorbent: $K_A = 2.67$, $K_B = 1$, $K_D = 2.21$, $y_A^F = y_B^F = 0.45$, $y_D^F = 0.1$, $\Omega_H = 1.38$, $\Omega_G = 2.29$. (b) Weak desorbent: $K_A = 2$, $K_B = 1$, $K_D = 0.8$, $y_A^F = y_B^F = 0.4$, $y_D^F = 0.2$, $\Omega_H = 0.85$, $\Omega_G = 1.39$. (c) Strong desorbent: $K_A = 2$, $K_B = 1$, $K_D = 2.5$, $y_A^F = 0.2$, $y_B^F = 0.6$, $y_D^F = 0.2$, $\Omega_H = 1.48$, $\Omega_G = 2.26$.

$$\text{point } C \quad \left(\frac{\Omega_G}{K_D}, \frac{\Omega_G}{K_D}\right) \tag{15}$$

$$\text{point } D \quad \left(\frac{\Omega_H}{K_D}, \frac{\Omega_H}{K_D}\right) \tag{16}$$

$$\text{point } R \quad \left(\frac{\Omega_H[\Omega_G(K_A - K_B) - \Omega_H(K_A - \Omega_G)]}{K_A K_D(\Omega_G - K_B)}, \frac{\Omega_H^2}{K_B K_D}\right) \tag{17}$$

$$\text{point } T \quad \left(\frac{\Omega_G^2}{K_A K_D}, \frac{\Omega_G[\Omega_H(K_A - K_B) - \Omega_G(\Omega_H - K_B)]}{K_B K_D(K_A - \Omega_H)}\right) \tag{18}$$

$$\text{point } W \quad \left(\frac{\Omega_G \Omega_H}{K_A K_D}, \frac{\Omega_G \Omega_H}{K_B K_D}\right) \tag{19}$$

$$\text{point } W_w \quad \left(\frac{K_B \Omega_G}{K_A K_D}, \frac{\Omega_G[\Omega_H(K_A - K_B) - K_B(\Omega_H - K_B)]}{K_B K_D(K_A - \Omega_H)}\right) \tag{20}$$

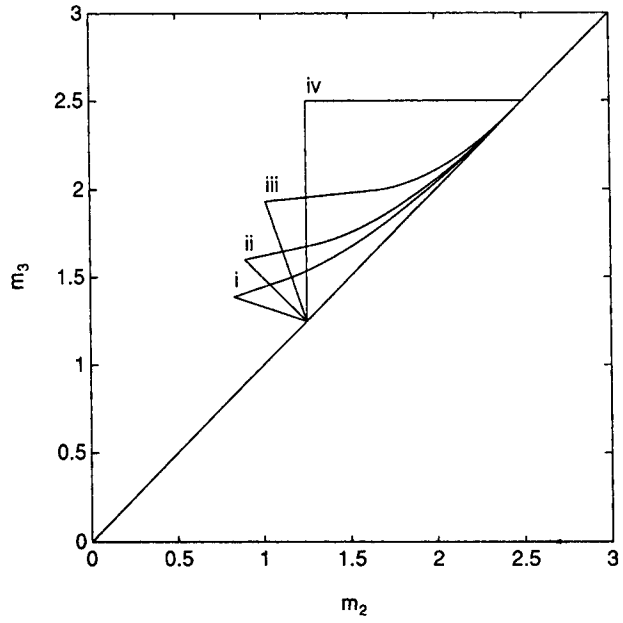


(a)

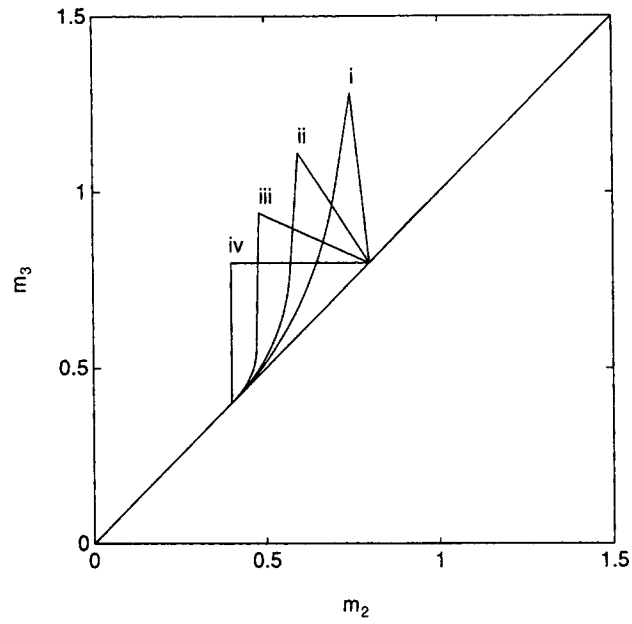


(b)

**Figure 3. Effect of the desorbent content in the feed on the region of complete separation in the ($m_2$, $m_3$) plane.**

(a) Weak desorbent: $K_A = 2$, $K_B = 1$, $K_D = 0.8$, $y_B^F/y_A^F = 1$. (b) Strong desorbent: $K_A = 2$, $K_B = 1$, $K_D = 2.5$, $y_B^F/y_A^F = 3$. (i) $y_D^F = 0$; (ii) $y_D^F = 0.33$; (iii) $y_D^F = 0.66$; (iv) $y_D^F \to 1$, that is, linear system.

$$\text{point } W_s \quad \left( \frac{\Omega_H[\Omega_G(K_A - K_B) - K_A(K_A - \Omega_G)]}{K_A K_D(\Omega_G - K_B)}, \frac{\Omega_H K_A}{K_B K_D} \right). \tag{21}$$

It is noteworthy that the coordinates of all these points depend not only on the equilibrium constants of the involved components but also on the parameters $\Omega_H$ and $\Omega_G$ representing the lower and upper root, respectively, of the following quadratic equation (which has only real and positive solutions, and hence $\Omega_G > \Omega_H > 0$):

$$\delta_F \Omega^2 - [K_A y_A^F(K_B + K_D) + K_B y_B^F(K_A + K_D) + K_D y_D^F(K_A + K_B)]\Omega + K_A K_B K_D = 0, \tag{22}$$

where

$$\delta_F = K_A y_A^F + K_B y_B^F + K_D y_D^F. \tag{23}$$

The points inside the complete separation region in Figures 2a, 2b and 2c represent values of the operating parameters $m_2$ and $m_3$ for which in the frame of Equilibrium Theory complete separation is achieved, provided that the conditions on $m_1$ and $m_4$ reported earlier are also satisfied.

## Effect of the Desorbent on the Separation Performance

It can readily be shown that when the feed contains no desorbent, that is, when $y_D^F = 0$, all of the preceding equations reduce to the corresponding ones reported by Mazzotti et al. (1994). In this case, one of the roots of Eq. 22 equals $K_D$, whereas the other one equals $\Omega_F = K_A K_B/(K_A y_A^F + K_B y_B^F)$. Since it can be either $\Omega_F > K_D$ or $\Omega_F < K_D$, two distinct cases corresponding to either condition were considered in the analysis reported by Storti et al. (1993) for the case of intermediate desorbent. In this work we have shown, by letting $y_D^F \geq 0$, that these actually represent two special cases of a much more general class constituted of separations where the feedstream consists of $A$, $B$, and $D$. Therefore, we develop criteria for the design of operating conditions to achieve complete separation that allow for the presence of some desorbent in the feed. This yields both a generalization of the results obtained in previous parts of this work as well as a significant simplification of the relationships to be used in the case of intermediate desorbent.

Let us now analyze the effect of the presence of the desorbent in the feed on the separation performance. This is illustrated in Figure 3, where the complete separation regions for the same system, that is, same ratio between mole fractions of $A$ and $B$ in the feed, are shown for various values of the desorbent mole fraction in the feed mixture. In particular, the cases of strong and weak desorbent are considered in Figures 3a and 3b, respectively. In both instances four complete separation regions are shown, going from region (i), corresponding to the case of a desorbent-free feedstream, to region (iv), which corresponds to the limiting situation of a feed mixture constituted of $A$ and $B$ infinitely diluted in the desorbent itself. In this last case, the concentrations of $A$ and $B$ are so small in the whole separation unit that the stoichiometric Langmuir model (Eq. 2) reduces to $\theta_i = K_i y_i/K_D$, which corresponds to a linear equilibrium model with $H_i = K_i/K_D$. Accordingly, introducing these values in Eq. 3 yields the same complete separation regions (iv) shown in Figures 3a and 3b, that is, a right triangle. It is worth noticing that defining the desorbent-free mole fractions of components $A$ and $B$ in the feed, that is, $\xi_i^F = y_i^F/(1 - y_D^F)$ with $i = A$, $B$,

yields the following expression for the value of the parameter $\Omega_F$: $\Omega_F = K_A K_B/(K_A \xi_A^F + K_B \xi_B^F)$. The straightforward consequence that $\Omega_F$ does not change with $y_D^F$ will be exploited in the following.

Several insights about the separation performance that are of direct relevance for the applications can be drawn from the results shown in Figure 3. The basis of the triangle-shaped region—the segment $AB$—remains the same, whereas the position of the vertex $W$ moves. This movement is downwards to the left in the case of strong desorbent, while it becomes the opposite, that is, upwards to the right, for a weak desorbent. In the case of intermediate desorbent either behavior is possible, depending on the relative position of the vertex of the region in the case where no desorbent is present in the feed, that is, the point $(\Omega_F/K_A, \Omega_F/K_B)$, and that of the linear region, that is, the point $(K_B/K_D, K_A/K_D)$. If these two points coincide, then the vertex remains in the same position and only the shape of the region changes. This very specific situation occurs for $K_D = K_A K_B/\Omega_F$ and is illustrated in Figure 4.

From the point of view of the design of the optimal separation these results have very clear implications, since the vertex $W$ represents the optimal operating conditions, in terms of both desorbent requirement and adsorbent utilization (Storti et al., 1995). Therefore, we can draw the following general conclusions about how to modify the operating conditions in order to maintain optimal separation when the desorbent content in the feed changes:

1. Increasing amounts of the strong desorbent in the feed stream call for decreasing values of the fluid to solid flow-rate ratio both in sections 2 and 3.

2. Increasing amounts of the weak desorbent in the feedstream require increasing values of parameters $m_2$ and $m_3$.

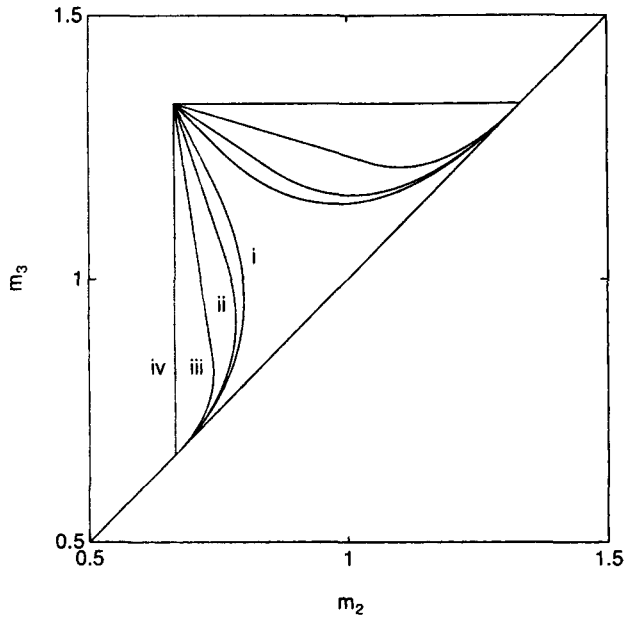


**Figure 4. Effect of the desorbent content in the feed on the region of complete separation in the ($m_2$, $m_3$) plane for the case $K_D = K_A K_B/\Omega_F$.**

$K_A = 2$, $K_B = 1$, $K_D = 1.5$, $y_B^F/y_A^F = 1$. (i) $y_D^F = 0$; (ii) $y_D^F = 0.1$; (iii) $y_D^F = 0.4$; (iv) $y_D^F \to 1$, that is, linear system.

3. The presence of an intermediate desorbent in the feedstream has an effect on the separation performance that is similar to that of a strong or a weak desorbent (as described), depending on whether $K_D > K_A K_B/\Omega_F$ or $K_D < K_A K_B/\Omega_F$, respectively. The case where $K_D = K_A K_B/\Omega_F$ corresponds to no movement of the optimal operating point, as illustrated in Figure 4.

Another important issue in applications refers to the robustness of the separation. By this we mean that after a small perturbation of the operating conditions the unit changes its quantitative performance but still achieves complete separation, that is, it does not modify its qualitative behavior (Storti et al., 1993). This aspect is rather critical for this kind of separation, since the optimal operating conditions are typically not robust because close to its vertex, which is the optimal operating point, the triangle may be very thin. Figures 3a and 3b show that increasing the desorbent content in the feed produces an increase in the angle between the two straight lines $WD$ and $WC$, both in the case of strong and weak desorbent. Since this *angle* may be taken as a measure of the robustness of the separation in the optimal region (i.e., close to the vertex), this means that the robustness itself increases when $y_D^F$ increases. This effect is illustrated in Figure 5, where the amplitude of the angle just mentioned is plotted as a function of the mole fraction of the desorbent in the feed mixture. It can be observed that for all types of desorbent considered, the angle, and hence the separation robustness, increases when $y_D^F$ increases. As shown in the figure and demonstrated by several calculations not reported here, the shape of this curve depends on the specific values of the

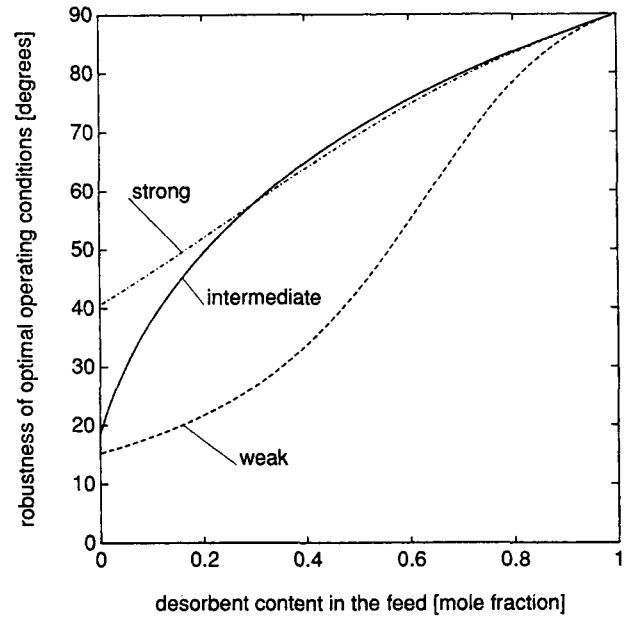


**Figure 5. Effect of the desorbent content in the feed on the amplitude of the angle between the two straight lines passing through the vertex of the region of complete separation in the ($m_2$, $m_3$) plane.**

This amplitude is a measure of the robustness of the optimal separation conditions. $K_A = 2$, $K_B = 1$, $y_A^F/y_D^F = 1$. (—), intermediate desorbent, $K_D = 1.5$; (- -), weak desorbent, $K_D = 0.5$; (- · -), strong desorbent, $K_D = 3$.

equilibrium constants and on the ratio between the mole fractions of components $A$ and $B$ in the feed mixture. However, the following conclusion bears instead full generality:

4. Increasing amounts of desorbent (strong, weak, or intermediate) in the feedstream lead to increasingly robust optimal operating conditions.

The behavior of the separation robustness discussed earlier can be even better appreciated in the special case shown in Figure 4 where $K_D = K_A K_B/\Omega_F$, and hence the vertex of the triangle does not move when changing the desorbent content in the feed. It is worth stressing that this feature is true only for this particular example, which has been selected only to make more evident the comparison of shapes and areas of complete separation regions corresponding to different values of $y_D^F$. The increase in robustness of the operating conditions corresponding to higher values of $y_D^F$ is evident in terms of both the area of the complete separation regions and the angle between the two straight lines $WD$ and $WC$. It is worth noticing that when $y_D^F$ goes from 0 to 0.1, the angle increases from 41° to 46°, which corresponds to a 13% increase in robustness of the optimal separation, that is, for an operating point in the region close to the vertex. When $y_D^F = 0.4$, the angle is 64°, corresponding to a 56% increase in robustness.

Finally, it is worth mentioning that the qualitative behavior of the separation performance for different values of the desorbent content in the feed discussed earlier is expected to apply also to other separations besides that of binary mixtures described by the stoichiometric Langmuir isotherm discussed in this work. These include multicomponent mixtures and systems characterized by the nonstoichiometric Langmuir isotherm.

## Comparison with Experimental Results: SMB Enantiomer Separation

The theoretical results discussed earlier can be assessed by comparison with some experimental data obtained in a 12-port simulated moving-bed pilot unit by Küsters et al. (1995). These refer to the separation on the chiral stationary phase Chiralcel-OD of the racemic epoxide (±)-1*a*,2,7,7*a*-tetrahydro-3-methoxynaphth-(2,3*b*)-oxirene, which is an intermediate in the asymmetric synthesis of some optically active drugs.

First, we have fitted the experimental adsorption equilibrium data reported in the original article using the stoichiometric Langmuir isotherm (Eq. 2). To this aim the reference value $K_D = 1$ has been attributed to the equilibrium constant of the desorbent, an *n*-hexane/*iso*-propanol 9/1 mixture, about whose adsorption properties no information is available. As illustrated in Figure 6, a good agreement between experimental and calculated isotherms is achieved using the parameters $\rho_s \Gamma^\infty = 175$ kg/m$^3$, $K_A = 21$, and $K_B = 16$, where the subscripts $A$ and $B$ refer to the (−) and the (+) enantiomer, respectively. Note that the agreement is very good for concentrations smaller than 10 kg/m$^3$, which is the range considered in the SMB experiments, whereas it becomes rather poor outside this range. The values of the equilibrium constants $K_j$, $j = A, B$ represent the selectivities of the relevant species with respect to the desorbent and their obtained values indicate that, as expected, the affinity of the solvent for the chiral stationary phase is very small with respect to that of the two enantiomers.

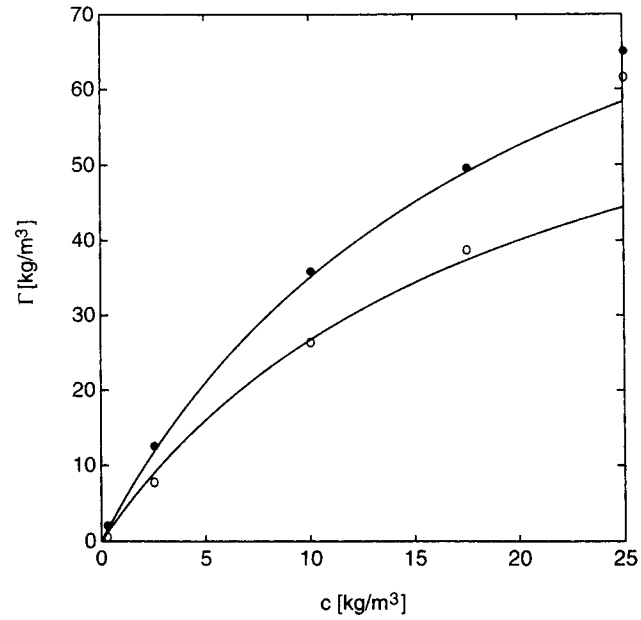


**Figure 6. Experimental (from Küsters et al., 1995) and calculated adsorption isotherms for the epoxide enantiomers on Chiralcel-OD.**

●: (−) enantiomer; ○: (+) enantiomer.

Now, let us consider the SMB experiments. The corresponding geometric and operating parameters are as follows: $AL = 20.1 \times 10^{-6}$ m$^3$; $\epsilon^* = 0.67$; $\rho_f = 700$ kg/m$^3$; $t^* = 780$ s. Three experiments are reported, performed at two different racemate concentration levels, namely, a low and a high level corresponding to 5 and 20 kg/m$^3$, respectively. Applying the theory developed in the previous sections, two different complete separation regions in the $(m_2, m_3)$ plane can be calculated, using the feed concentrations $y_A^F = y_B^F = 2.5/700$ (region $S$) and $y_A^F = y_B^F = 10/700$ (region $G$), respectively. These are drawn in Figure 7, together with the complete separation region corresponding to the case of infinite dilution of the feed mixture (region $L$), that is, corresponding to the linear behavior of the system, and with the operating points representing the experimental runs as calculated using Eq. 1. The values of the operating flow rate ratios $m_j$ are reported in Table 1, together with the experimental values of feed concentrations and purities of the extract and raffinate streams. Note that runs 1 and 2 share the same operating point, but with different values of the feed concentration. Since the desorbent is weak, the critical value of the parameter $m_4$ is not constant, but it must be calculated as a function of all the other flow-rate ratios specifically for each experimental run (cf. the discussion of Eqs. 4 and 5). These critical values are reported in brackets next to the experimental values of $m_4$.

It can readily be noticed that in all the experimental runs the operating values of $m_1$ and $m_4$ fulfill the relevant constraint, which is given by Eq. 4 for the former and has just been discussed for the latter. Now, let us consider the relative position of the operating points in Figure 7 with respect to the predicted regions of complete separation. In particular, the position of point 1 must be compared with the complete separation region $S$, corresponding to the smaller feed concentration, whereas the position of points 2 and 3 with

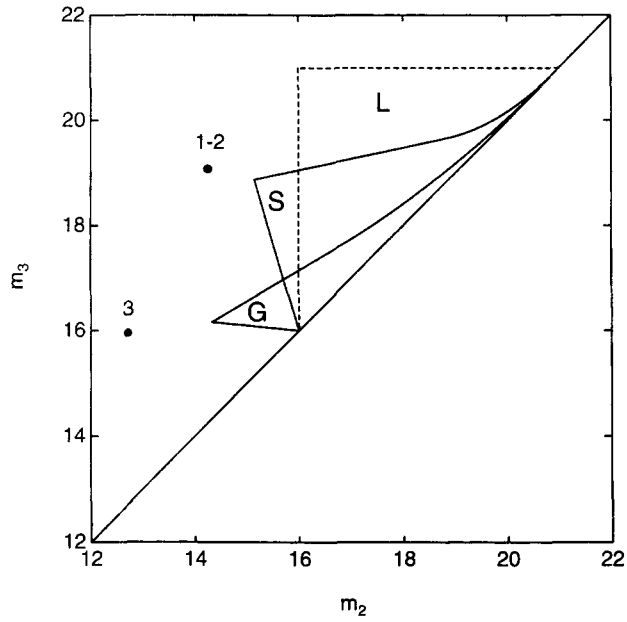


**Figure 7. Comparison of the predicted regions of complete separation in the ($m_2$, $m_3$) plane with the experimental data (●).**

Region L (dashed boundaries): linear region of complete separation; region S: 5 kg/m$^3$ of racemate feed concentration; region G: 20 kg/m$^3$. The position of point 1 must be compared with region S, whereas those of points 2 and 3 must be compared with region G.

the complete separation region $G$, corresponding to the greater feed concentration.

No operating point belongs to the relevant complete separation region. In particular, point 1 is in the region where neither outlet stream is pure, but it is very close to the optimal operating point of the corresponding complete separation region $S$. This compares well with the experimental performance achieved during run 1, where purities between 96 and 98% have been obtained in both the extract and the raffinate. The situation is similar in the case of run 3 (consider the position of the operating point 3 with respect to the separation region $G$), and in fact also in this case very large purity values have been achieved, that is, around 95%. Let us now consider run 2: changing the feed concentration from 5 to 20 kg/m$^3$ produces a rather large shift of the complete separation region (from region $S$ to region $G$), which leaves the operating point 2, coincident with operating point 1, in the region of the ($m_2$, $m_3$) plane where the raffinate purity drops sharply. This is in full agreement with the experimental measurements that indicate a fall of raffinate purity from 96.5% in run 1 to 43% in run 2.

The observed fall in separation performance is normally attributed to the transition of the system from linear to nonlinear behavior. The theoretical analysis and the experimental results presented in this work demonstrate that this is indeed the case. As shown in Figures 3, 4, and 7, the complete separation region moves gradually further and further away from the linear region while the feed concentration is increased. Accordingly, when the feed concentration increases, the operating conditions must be changed in order to maintain the same separation performance of the system. The design criteria developed in this work provide one with reliable guidelines for performing the correct choice of optimal and robust operating conditions whatever the concentration of the feed stream is.

**Table 1. Separation of the Chiral Epoxide: Flow-Rate Ratios and Separation Performances of the Experimental Runs***

| Run | Feed Racemate Conc. (kg/m$^3$) | Flow-Rate Ratios | | | | Experimental Purity Values | |
|---|---|---|---|---|---|---|---|
| | | $m_1$ | $m_2$ | $m_3$ | $m_4$ ($m_{4,cr}$) | $P_E$ (%) | $P_R$ (%) |
| 1 | 5 | 22.1 | 14.3 | 19.0 | 11.1 (15.2) | 98.2 | 96.5 |
| 2 | 20 | 22.1 | 14.3 | 19.0 | 11.1 (13.2) | 93.8 | 43.0 |
| 3 | 20 | 22.1 | 12.7 | 15.8 | 9.6 (12.9) | 94.4 | 95.0 |

*Source: Küsters et al., 1995.
The critical value of the flow-rate ratio in the fourth section, $m_{4,cr}$, is reported in brackets next to the operating value, $m_4$.

## Notation

$A$ = cross section of the adsorption column
$c_i$ = fluid-phase molar (or mass) concentration of component $i$
$f_i^j$ = dimensionless net flow rate of component $i$ in section $j$, $f_i^j = m_j y_i^j - \theta_i^j$
$G_j$ = fluid molar (or mass) flow rate in section $j$ of an SMB unit
$H_i$ = Henry constant of component $i$
$L$ = length of subsection in an SMB unit
$NC$ = total number of components
$t^*$ = switching time in an SMB unit
$u_j$ = superficial fluid-phase velocity in section $j$
$u_s$ = superficial solid-phase velocity
$y_i$ = fluid-phase dimensionless concentration of component $i$, $y_i = c_i/\rho_f$
$\Gamma_i$ = molar (or mass) concentration of component $i$ per unit mass of solid
$\Gamma_i^\infty$ = saturation molar (or mass) concentration of component $i$ per unit mass of solid
$\Gamma^\infty$ = reference molar (or mass) concentration per unit mass of solid
$\delta$ = denominator in the Langmuir isotherm (Eq. 2).
$\epsilon$ = external void fraction
$\epsilon_p$ = intraparticle void fraction
$\epsilon^*$ = overall void fraction, $\epsilon^* = \epsilon + \epsilon_p(1-\epsilon)$
$\rho_f$ = fluid-phase reference molar (or mass) density
$\rho_s$ = bulk solid mass density

### *Subscripts and superscripts*

$A, B$ = components to be separated ($K_A > K_B$)
$D$ = desorbent
$E$ = extract
$F$ = feed
$i$ = component index
$j$ = section index
$l$ = component index
$R$ = raffinate

## Literature Cited

Baciocchi, R., M. Mazzotti, G. Storti, and M. Morbidelli, "$C_5$ Separation in a Vapor Phase Simulated Moving Bed Unit," *Fundamentals of Adsorption*, M. D. LeVan, ed., Kluwer Academic Publishers, Boston (1996).

Charton, F., and R.-M. Nicoud, "Complete Design of a Simulated Moving Bed." *J. Chromatog. A*, **702,** 97 (1995).

Ching, C. B., K. H. Chu, K. Hidajat, and M. S. Uddin, "Comparative Study of Flow Schemes for a Simulated Countercurrent Adsorption Separation Process," *AIChE J.*, **38,** 1744 (1992).

Ching, C. B., B. G. Lim, E. J. D. Lee, and S. C. Ng, "Preparative Resolution of Praziquantel Enantiomers by Simulated Counter-Current Chromatography," *J. Chromatog.*, **634,** 215 (1993).

Ching, C. B., and D. M. Ruthven, "An Experimental Study of a Sim-

ulated Counter-Current Adsorption System: I. Isothermal Steady-State Operation, *Chem. Eng. Sci.*, **40,** 877 (1985).
Ganetsos, G., and P. E. Barker, eds., *Preparative and Production Scale Chromatography*, Marcel Dekker, New York (1993).
Helfferich, F., "The *h*- and $\omega$-Transformations in Multicomponent Fixed-Bed Ion Exchange and Adsorption: Equivalent Mathematics, Different Scope," *Chem. Eng. Sci.*, **46,** 3320 (1991).
Helfferich, F., and G. Klein, *Multicomponent Chromatography: Theory of Interference*, Marcel Dekker, New York (1970).
Küsters, E., G. Gerber, and F. D. Antia, "Enantioseparation of a Chiral Epoxide by Simulated Moving Bed Chromatography using Chiralcel-OD," *Chromatographia*, **40,** 387 (1995).
Mazzotti, M., G. Storti, and M. Morbidelli, "Robust Design of Countercurrent Adsorption Separation Processes: 2. Multicomponent Systems," *AIChE J.*, **40,** 1825 (1994).
Mazzotti, M., G. Storti, and M. Morbidelli, "Robust Design of Countercurrent Adsorption Separation Processes: 3. Nonstoichiometric Systems," *AIChE J.*, **42,** 2784 (1996).
Negawa, M., and F. Shoji, "Optical Resolution by Simulated Moving-Bed Adsorption Technology," *J. Chromatog.*, **590,** 113 (1992).
Nicoud, R.-M., G. Fuchs, P. Adam, M. Bailly, E. Küsters, F. D. Antia, R. Reuille, and E. Schmid, "Preparative Scale Enantioseparation of a Chiral Epoxide: Comparison of Liquid Chromatography and Simulated Moving Bed Adsorption Technology," *Chirality*, **5,** 267 (1993).
Rhee, H.-K., R. Aris, and N. Amundson, "Multicomponent Adsorption in Continuous Countercurrent Exchangers," *Philos. Trans. Roy. Soc. London*, **A269,** 187 (1971).
Ruthven, D. M., *Principles of Adsorption and Adsorption Processes*, Wiley, New York (1984).
Ruthven, D. M., and C. B. Ching, "Counter-Current and Simulated Counter-Current Adsorption Separation Processes," *Chem. Eng. Sci.*, **44,** 1011 (1989).
Storti, G., R. Baciocchi, M. Mazzotti, and M. Morbidelli, "Design of Optimal Operating Conditions of Simulated Moving Bed Adsorptive Separation Units," *Ind. Eng. Chem. Res.*, **34,** 288 (1995).
Storti, G., M. Mazzotti, M. Morbidelli, and S. Carrà, "Robust Design of Binary Countercurrent Adsorption Separation Processes," *AIChE J.*, **39,** 471 (1993).

## Appendix

In this Appendix we provide an outline of the procedure followed to derive Eqs. 6 to 21. Here we describe in detail only the case of intermediate desorbent, thus generalizing the analysis reported by Storti et al. (1993) for desorbent-free feedstreams. The extention to weak and strong desorbents can be performed following the same procedure developed by Mazzotti et al. (1994), again in the context of desorbent-free feedstreams.

It can be readily observed that the conditions for complete separation reported by Storti et al. (1993) also apply in the case examined in this work. These are given in terms of equilibrium constants, mole fractions of $A$ and $B$ in the feed, and $m_2$ and $m_3$ as follows:

$$b_2 - \sqrt{b_2^2 - 4c_2} > b_1 - \sqrt{b_1^2 - 4c_1} \tag{A1}$$

$$b_2 + \sqrt{b_2^2 - 4c_2} > b_1 + \sqrt{b_1^2 - 4c_1} \tag{A2}$$

$$b_2^2 - 4c_2 > 0 \tag{A3}$$

$$b_1^2 - 4c_1 > 0 \tag{A4}$$

$$m_3 > m_2, \tag{A5}$$

where

$$b_1 = K_B + K_D m_3 - (K_D - K_B) y_B^F (m_3 - m_2), \tag{A6}$$

$$c_1 = K_B K_D m_3, \tag{A7}$$

$$b_2 = K_A + K_D m_2 - (K_A - K_D) y_A^F (m_3 - m_2), \tag{A8}$$

$$c_2 = K_A K_D m_2. \tag{A9}$$

These constraints define a region in the $(m_2, m_3)$ plane constituted of points corresponding to operating conditions that, in the frame of equilibrium theory, allow us to achieve complete separation, provided that conditions 4 and 5 on $m_1$ and $m_4$ are fulfilled.

It is worth noting that Eqs. A1 to A5 implicitly account for complete separation conditions, with no assumption whatsoever about the presence of the desorbent in the feed mixture, whose mole fraction can be zero or nonzero, that is, $y_D^F \geq 0$.

Differences due to the value of the parameter $y_D^F$ arise when, starting from the preceding conditions, explicit expressions for the boundaries of the complete separation region are derived. For this, the procedure described in Appendix D by Storti et al. (1993) applies only when $y_D^F = 0$. The more general case considered here, that is, the case where $y_D^F \geq 0$, can be dealt with through a similar procedure, although the detailed algebraic manipulations are necessarily different. An example of this is that by summing Eqs. A1 and A2, the necessary conditions for complete separation $b_2 \geq b_1$ are obtained. Using Eqs. A6 and A8, the previous inequality yields the following constraint:

$$m_3 - m_2 \leq \frac{K_A - K_B}{K_A y_A^F + K_B y_B^F + K_D y_D^F}, \tag{A10}$$

which reduces to Eq. D1 of Storti et al. (1993) when $y_D^F = 0$.

Thus, after some algebraic manipulations, Eqs. 6, 7, 10, 11, and 12 are obtained, which are consistent with the results reported in the cited paper for the special case where $y_D^F = 0$.

*Manuscript received Mar. 4, 1996, and revision received June 24, 1996.*